Cairo University

المؤتمر الدولى التاسع لهندسة المناجم و البترول و الفلزات
The 9th International International Mining, Petroleum, and Metallurgical Engineering Conference

MPM

EL SELLA SHEAR ZONE, SOUTHEASTERN DESERT, EGYPT; AN EXAMPLE OF VEIN-TYPE URANIUM DEPOSIT

M.E. Ibrahim*, A.A. Zalata, H.S. Assaf*, I.H. Ibrahim* and M.A. Rashed***

*Nuclear Materials Authority, Cairo, Egypt.
** Geology Department, Faculty of Science, Mansoura University, Mansoura, Egypt.

ABSTRACT:

EL Sella granitoid rocks comprise biotite tonalite, two-mica monzogranite and muscovite monzogranite. The biotite tonalite and two-mica monzogranite originated from metaluminous and peraluminous magma respectively. The two-mica monzogranites (G. El Sella) resemble continental-collision granitoids and emplaced during syn-collision regime whereas the biotite tonalites resemble island-arc granitoids. The muscovite monzogranite (G. Qash Amir) is affected by deutric alteration and characterized by gradational contact with two-mica monzogranite, peraluminous in nature with visible primary and secondary uranium minerals, beryl and columbite.

The two-mica monzogranite is dissected by major continuous shear zone (ENE-WSW) extending for about 1560 m in length (2-40 m in width) and dips 70° due to SSE. El Sella shear zone is subdivided by two wrench faults (N15^{o}W-S15^{o}E) into three separated parts. Three generations of milky quartz (barren) veins are common; the oldest one, at the shear margins parallel to the shear zone, and dissected by two young generations with obvious displacement. Red and grey jasperoid (mineralized) veins are also common parallel to both the shear zone and milky quartz vein generation, with visible pyrite and secondary U-minerals. Argillization, fluoritization, hematitization, silicification, carbonization and sulphidization are the main alteration processes.

The U migrated out from G. Qash Amir (muscovite monzogranites), G. El Sella (two-mica monzogranites) and biotite tonalites to the shear zone. In contrast, the shear zone acts as a good trap for the previous migrated uranium. Inside the shear zone itself, the jasper veins and argillic fine-grained granites gain uranium, whereas hematite fine-grained granites loss uranium.

INTRODUCTION

Uranium deposits world-wide can be grouped into four major categories of deposit types based on the geological setting of the deposits [1]; 1- unconformity-related deposits, 2- breccia complex deposits, 3- sandstone deposits, 4- surficial deposits, 5- volcanic deposits, 6- intrusive deposits, 7- metasomatite deposits, 8- metamorphic deposits, 9- quartz-pebble conglomerate deposits and 10- vein deposits.

The basic principles for the formation of U-deposits [2] are; 1- mobilized source, 2- transportation, 3- deposition, 4- reconcentration and 5- preservation. Two main types of fertile granites (U content > 10 ppm, Th/U ratio <2) are associated with U-deposits can be distinguished; peraluminous leucogranites (enriched in K, Rb, Li, F, Sn, W but poor in Th, REE and Zr) and metaluminous or weakly peraluminous granites (enriched in K, Rb, F, Sn, W, Th, REE and Zr).

No typical vein-type U-deposits cross-cut two-mica peraluminous granites have been recorded before in Egypt except El Sella shear zone. The objective in this study is to test the difference between the two-mica monzogranite and the muscovite monzogranite as well as shed some lights on El Sella shear zone from the geologic and spectrometric points of view.

GEOLOGIC SETTING AND PETROGRAPHY

The rocks in the study area are represented by (from older to younger) ophiolitic assemblage (antigorite serpentinite, metapyroxenite, metagabbro) amphibolite), mélange matrix (biotite-muscovite schist, actinolite schist and quartzo-feldspathic schist), older granite (biotite tonalite), Dokhan volcanics (andesites and dacites), molasse (Hammamat) sediments, younger granites (two-mica monzogranite and muscovite monzogranite) and post granite dykes (Fig. 1). The two-mica monzogranite is dissected by two-shear zones perpendicular on each others, (ENE-WSW and NNW-SSE) (Fig. 2). The results of modal analysis of the studied granitic samples are plotted graphically in QAP triangular diagram [3]. The figure indicates that both G. El Sella and G. Qash Amir granitic rocks are mainly monzogranites (Fig. 3).

A- Biotite tonalite

Biotite tonalite pluton in the area under investigation constitutes a small mass (1.0 km^2), cropping out at the southeastern part and extends further southward beyond the limits of the mapped area (Fig. 1). It occurs as low lying country that often dissected by small intermediate dykes. This rock is generally homogenous in its mineralogical composition, but in general, it shows gradual increase of mafic minerals as we approach to its contact with Dokhan volcanics. The biotite tonalites are highly fractured, jointed (N-S and ENE-WSW) and containing semi-rounded xenoliths of mafic composition. The latter reach up to 15 x 20 cm across which show varying degrees of assimilation. Epidote veinlets are common (2 cm thick), trending N30°W with an angle of dip 70° due to SW.

This rock is medium- to coarse-grained, grey in colour, highly jointed and fragmented. It is mainly composed of plagioclase, quartz, biotite and subordinate amount of potash feldspars. Secondary minerals include chlorite, epidote and sericite. Zircon, apatite and opaques are accessory minerals.

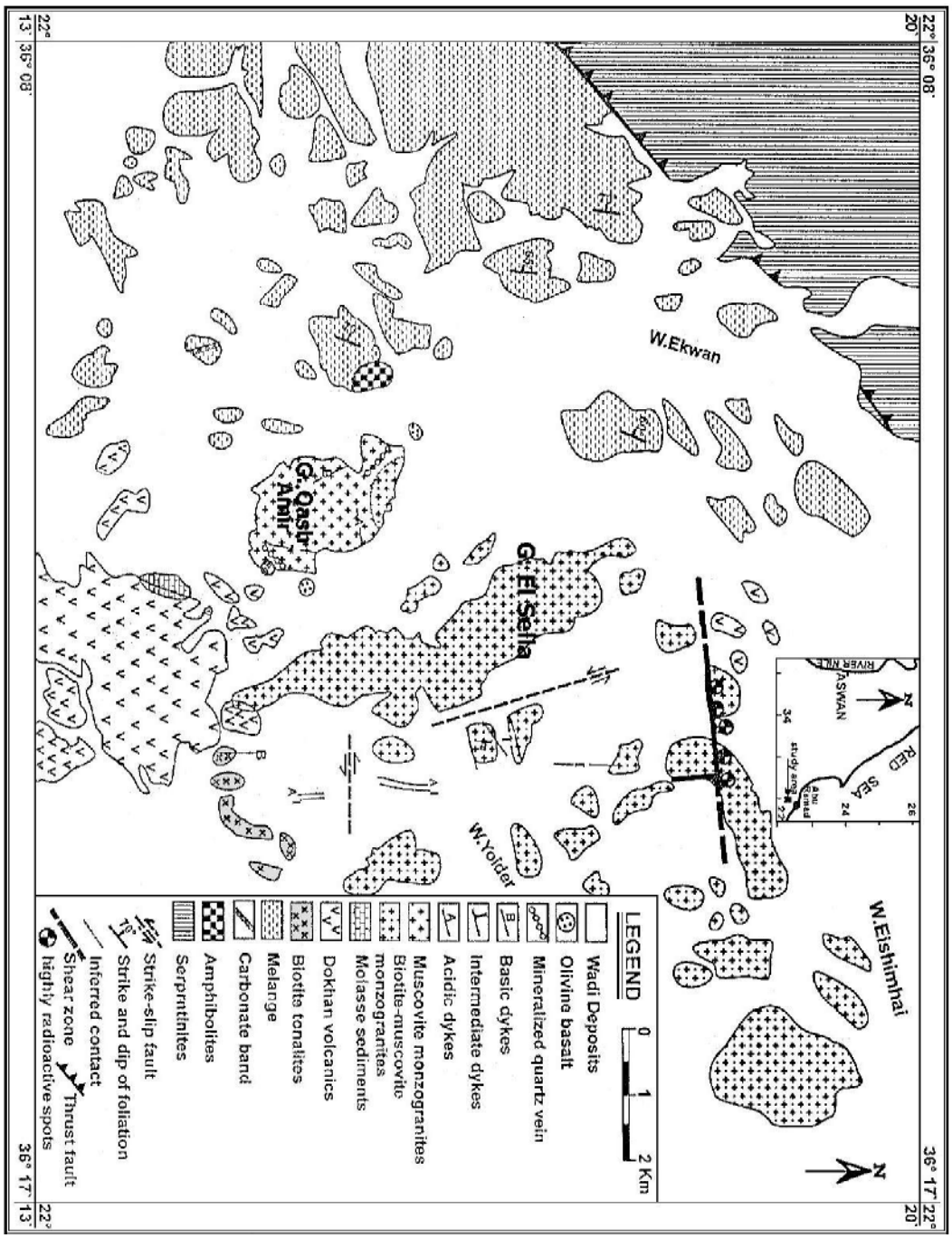

Fig. (1): Geologic map of G. Qash Amir and G. El Sella area, Southeastern Desert, Egypt.

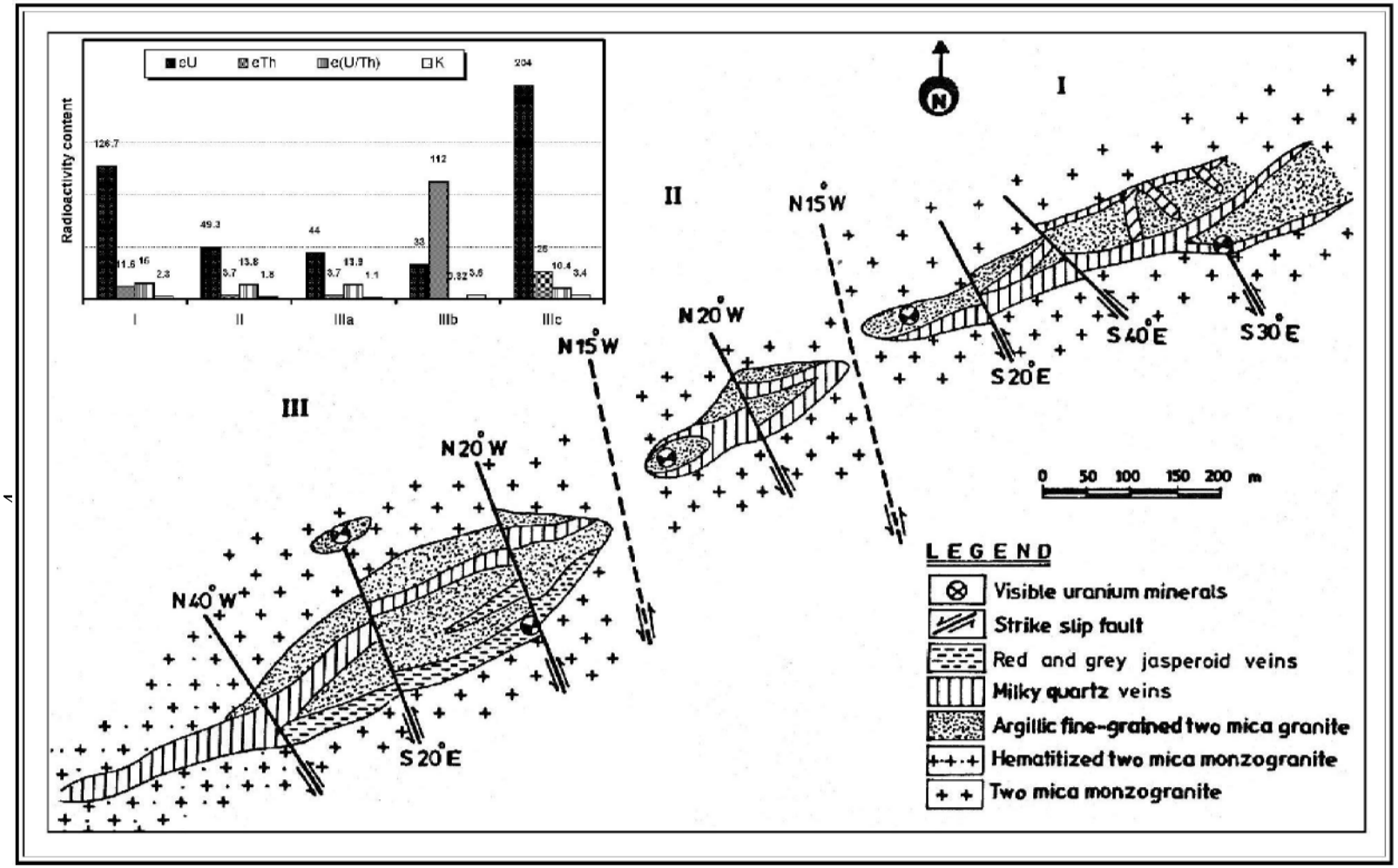

Fig. (2): Geologic map of El Sella shear zone.

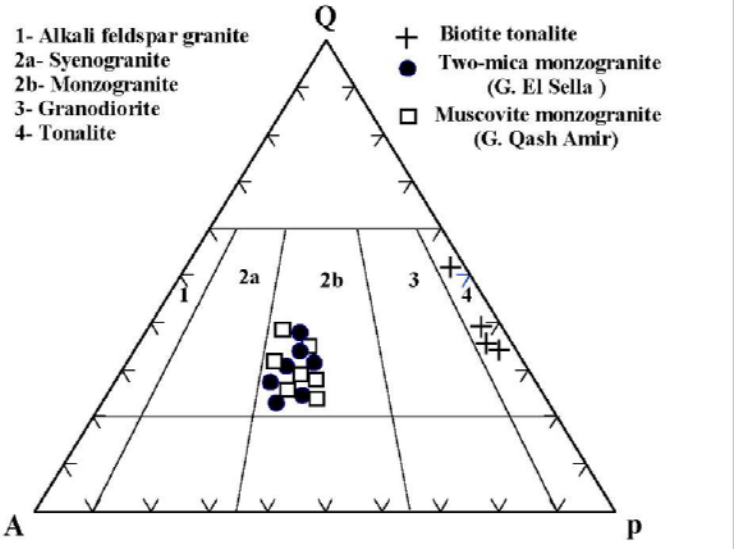

Fig. (3): Graphical plotting of modal analysis results on QAP triangular diagram [3].

B- Two-mica monzogranites (G. El Sella)

Gabal El Sella (two-mica monzogranite) is elongated in NNW direction (Fig. 1). These monzogranites occupy the major part of the studied area (100 Km^2) at the center and northeastern parts of the mapped area (Fig .1) varying in colours from red, pink to buff. They are usually fine- medium to coarse-grained and characterized by hypidiomorphic granitic texture. They are divisible into several bodies separated by sandy corridors with highest peaks rise to as high as 557 m (above sea level). It dissected by two shear zones (ENE-ESE and NNW-SSE). The ratio of muscovite to biotite in G. El Sella varies from place to another. Close to the major shear zone (ENE-WSW), muscovite decreases and biotite increases. On contrast, the reverse is true, when we go away from the major shear zone and becomes in close contact with G. Qash Amir muscovite monzogranite.

Microscopically, the two-mica monzogranite is composed mainly of quartz (34 in vol.%), potash feldspars (33 in vol.%), plagioclase (26 in vol.%), biotite and muscovite (4.5 in vol. %). Secondary minerals are kaolinite, sericite and chlorite. Zircon, apatite, monazite, garnet, and opaques are accessory minerals (2.5 in vol.%).

C- Muscovite monzogranites (G. Qash Amir)

G. Qash Amir (muscovite monzogranites) occurs as isolated hill, oval in shape and covering an area of about 3.0 Km^2. These rocks are medium- to coarse-grained, massive, pink in colour and hypidiomorphic in texture. They are characterized by minor xenoliths, exfoliated and cavernous external features due to subsequent weathering processes. At the peripheries of the pluton, Mn-mineralizations are filling N-S and E-W fracture planes. Garnet (spessartine 65 in vol.% and alamandine 35 in vol.%) is very common in Qash Amir muscovite monzogranite and decreased in G. El Sella Two-mica monzogranites until it disappears in its northern part (shear-zone). The pluton is invaded by mineralized semihorizontal quartz veins (50 cm in width, 20.0 m in length) trending NNW and NNE with angles of dip 10°/ENE and 10-5°/WNW respectively at both western and eastern side of the pluton. Most of these mineralizations in quartz veins are mainly tungsten minerals, green to violet fluorite, Mn-oxides, pyrite, galena, sphalerite,

silver and gold [4]. Also basic and acidic dykes (barren) invade Qash Amir muscovite monzogranites. Greisening processes at its peripheries are common with beryl and columbite (confirmed by XRD) especially associated with the albitized zone at the core of the pluton. The beryl is commonly zoned, fractured and greenish to pale yellowish in colour with lenses/width ratio ranges between 4:1 and 6:1 and recorded here for the first time. Visible primary and secondary uranium mineralizations (uraninite, uranophane, beta-uranophane and autunite) are mainly disseminated and along it's closed space fracture planes [5] especially at the pluton margins. Intermediate dykes (N-S in trend) show some high intensity of radioactivity (110 ppm eU and 30 ppm eTh) especially at the intersection of the two fault systems (N-S and E-W). It could be related to mobilization and leaching of disseminated uranium minerals from the Qash Amir granitic mass and being concentrated at open channel ways.

Microscopically, muscovite monzogranite are consist mainly of quartz (35.0 in vol.%), potash feldspars (32.0 in vol.%), plagioclase (27.0 in vol.%) and muscovite (4.0 in vol.%). Kaolinite, sericite are secondary minerals. Garnet, zircon, apatite, monazite and opaques are accessories (2.0 in vol.%).

D- El-Sella shear zone

El-Sella two-mica monzogranite is dissected by two-shear zones (5-40 m in width and 100-1560 m in length) perpendicular on each others, (ENE-WSW and NNW-SSE). These shear zones are mainly composed of sheared fine-grained two-mica monzogranite with muscovite increment at the expense of biotite. They are enriched by pyrite and visible secondary uranium minerals (uranophane and ß-uranophane [5]). Moreover, small quartz veinlets (1-5 cm thick) in various directions invade the shear zones.

The first shear zone (ENE-WSW) extends for about 1560 m in length (2-40 m in width) and dips 70° due to SSE (Fig. 2). From the structural point of view, this shear zone is cut and displaced into three separated parts by two NNW-SSE trending strike-slip faults (Fig. 2). Three generations of milky quartz (barren) veins are common; the oldest one, at the shear margins, trending parallel to the shear zone, and dissected by two young generations; NW-SE and N-S with obvious displacement. Red and grey jasperoid (mineralized) veins (0.5-3m thick, 50-400m length) are also common (ENE-WSW) parallel to both the shear zone and older milky quartz vein generation, with visible, pyrite and secondary U-minerals. Argillization, fluoritization, hematitization, silicification, carbonization and sulphidization are the main alteration processes.

Acidic dykes (Muscovite microgranite) as well as intermediate and basic dykes (amygdaloidal latite and amygdaloidal quartz dolerite respectively) characterized by vugs completely filled by calcite are dominant along ENE-WSW shear zone. The second shear zone (NNW-SSE) extends for a short distance (100m) and dips 80° due to ENE. Also latite (trachyandesite) dyke (chemical trap for uranium) (20-50cm thick) is invaded in parallel trend to the shear zone. Along the shear zone, the two-mica monzogranites are highly sheared, kaolinized and completely eroded. The intensity of radioactivity and mineralizations in the first shear zone are very common and more pronounced than the second one. No visible uranium mineralization is recorded in the fresh samples.

Petrographically, the rocks are fine-grained, mylonitic and yellowish white in colour. Microscopically, they are essentially composed of quartz, potash feldspar, plagioclase, muscovite and biotite. Secondary minerals are sericite, kaolinite and chlorite. Opaques and garnet are the accessory minerals.

SPECTROMETRIC STUDY

From the exploration point of view, the primary task of the ground spectrometric survey is the reorganization of areas where U concentrations have occurred. The portable GS-256 Spectrometer (made in Czechoslovakia), with NaI (Tl) detector of 75 x 75 mm^2, is used. The spectrometric data reveals that the most favourable host rock for uranium and thorium mineralization in the study area is El Sella shear zone, two-mica monzogranite and muscovite monzogranite. Results of the gamma-ray spectrometric survey are illustrated in Tables (1, 2 & 3).

A- Two-mica monzogranite (G. El Sella)

It exhibits a wide range of eU contents ranging from 5 – 26 ppm with an average of about 10.1 ppm, while eTh contents range from 16 – 33 ppm with an average of about 23.4 ppm. The eU/eTh ratios range from 0.18 – 0.91 with an average of about 0.44 (Table 1). Comparing the above mentioned values with others [6,7,8 and 9] indicate that, the granites of G. El Sella are higher in eU and eTh contents. The ratio eU/eTh, generally 0.44 which is slightly much than the ratio of the global average of granites 0.33 [10].

B- Muscovite monzogranite (G. Qash Amir)

It shows increased background radioactivity level giving eU contents range from 10 – 26 ppm with an average of about 17.5 ppm, while, eTh contents range from 10 – 25 ppm with an average of about 17.7 ppm. The eU/eTh ratios range from 0.5 – 1.75 with an average of about 1 (Table 1). Comparing the above mentioned values with that reported by[6] indicates that, the granite of Qash Amir is characterized by high eU, normal eTh and with wide range of eU/eTh ratios (0.5 – 1.75), the global range is 0.33 [10]. Minor randomly scattered small irregular anomalies area have radioelements content lying in the range of 28-125 average 50 ppm eU, and 19-35 average 24 ppm eTh with eU/eTh ratio varying between 1.5 and 3.57 average 1.6.

C- El Sella shear zone

1- The first part (500 m in length) is characterized by moderate relief, highly tectonized, kaolinization, argillization, hematitization with visible U-minerals and sulphides. The eU content ranges from 18 to 850 ppm with an average of about 126 ppm, whereas eTh content ranges from 1.8-89.0 ppm with an average of about 11.6 ppm. The e(U/Th) ratio ranges from 7-55 with an average about 15.0 K% ranges from 1 to 8.8% (Table 2).

2- The second part (230 m in length) is highly sheared, low relief, argillic and relatively narrow (3-6 m width). The eU and eTh contents range from 6-194 ppm and 0.8-9.3 ppm with an average of about 49.3 and 3.7 respectively. The e(U/Th) ratio ranges from 5.5-38 with an average of about 13.8. The K% ranges from 0.8-3.1% with an average of 1.8%.

3- The third part (830 m in length) is characterized by the presence of red and grey to black jasper veins cross-cutting the shear zone in the same direction (ENE-WSW). Also hematitization, carbonitization and argillization are common alteration features. Visible bright yellow secondary U-minerals are recorded in the jasper vugs. The eU and eTh contents in jasper veins range from 15-121 ppm and from 1.2-7.5 ppm with an average of 44 and 3.7 ppm respectively. The average e(U/Th) ratio is nearly the same for the second part (13.9), but the average of K% decreases (1.1%).

Table (1). Spectrometric analyses of the range and average contents of eU, eTh (in ppm) and K% in the different rocks.

Rock type		eU		eTh		eU/eTh	K%	n*
		Range	Average	Range	Average	Average		
Ophiolitic melange		0.0-0.2	0.1	0.1-0.3	0.2	0.5	0.2	5
Biotite tonalites		0.4-1.5	1.0	1.7-3.0	2.4	0.42	1.7	5
Dokhan volcanics	Andesites	1.0-3.0	2.0	3.0-4.0	3.5	0.59	0.9	6
	Dacites	3.0-7.0	4.0	4.0-5.0	4.5	0.89	1.3	6
Molasse sediments		1.0-3.5	2.0	3.0-4.5	3.8	0.53	1.5	4
Muscovite monzogranites (G. Qash Amir)		10.0-26	17.5	10.0-25	17.7	1	4.4	17
Two-mica monzogranites (G. El Sella)		5.-26	10.1	16.33	23.4	0.44	4.5	15

n* = number of analysis

Table (2). Averages and ranges of eU, eTh and K% contents in the shear zone, G. El-Sella area.

Shear zone		eU (ppm)	eTh (ppm)	e(U/Th)	K%
First part (500 m) (n=22)		126.7 18-850	11.6 1.8-89	15 7-55	2.3 1.0-8.8
Second part (230 m) (n=15)		49.3 6-194	3.7 0.8-9.3	13.8 5.5-38	1.8 0.8-3.1
Third part (850 m)	Jasper vein (n=10)	44 15-121	3.7 1.2-7.5	13.9 2-36.6	1.1 0.5-1.9
	Hematitization zone (n=6)	33 25-52	112 55-155	0.32 0.21-0.46	3.6 2.6-4.5
	Argillization zone (n=10)	204 29-991	26 2.6-136	10.4 4-12	3.4 0.7-11.2

n = number of analyses.

Table (3): Some statistical parameters including averages eUp, eTh, eU_o, eU_m and U_m ratio% for granitic rocks in the study area.

Rock name			eUp	eTh	eU_o	eU_m	U_m. ratio
Two-mica monzogranites (G. El Sella)			10.1	23.4	28	-18	180%
Muscovite monzogranites (G. Qash Amir)			17.5	17.7	21	-3.5	20%
Shear zone	I		126	11.6	14	+112	88.8%
	II		49.3	3.7	4.4	+44.9	91.1%
	III	a.	204	26	31	+173	Argill. (84%)
		b.	33	112	134.4	-101.4	Hematite (306%)
		c.	44.0	3.7	4.4	+39.6	Jasper (90%)
Biotite tonalite			1	2.4	2.9	-1.9	190%

eU_m= Migrated equivalent U.
U_m. ratio = Rate of mobilization of uranium.
a = argillic granite; b = hematitic granite; c = jasper veins.

The hematitic sheared two-mica monzogranite shows low eU, high eTh (eU = 25-52 ppm, with average 33, while eTh = 55-155 ppm with average 112 ppm), low e(U/Th) ratio (0.32) and high K% (3.6%). On contrast, the argillic-sheared granite shows high average eU contents (204 ppm) ranges from 29-991 ppm and low average eTh contents (26 ppm) (ranges from 2.6-136 ppm). The e(U/Th) ratios range from 4-12 (av. = 10.4) and K% ranges from 0.7-11.2 (av. = 3.4). Table (2).

The excavations revealed the increase of radioactivity all over the trench (up to 3000 ppm eU) faces in close contact to silica veinlets with steeply angle of dip (>75^{o}) or nearly vertical. Also visible secondary U-minerals appears and increased with depth sporadically on joint surface as well as replacing the oxidized sulphide and filling the vugs.

URANIUM MOBILIZATION AND MIGRATION

As indicated from Table (1), it is clear that the granitic rocks of both G. El Sella and G. Qash Amir exhibit eU/eTh ratios varying between 0.18-0.91 and average 0.44 for G. El Sella and varying between 0.5 - 1.75 with an average 1 for G. Qash Amir. These values are high compared to the [6], which is commonly are recorded as the average range for granites and indicating post magmatic redistribution processes. This is also evidenced by the variation diagram of eU and eTh with their ratios eU/eTh for the two masses (Figs. 4&5). The diagram illustrate that the eU/eTh ratio is directly proportional with eU, while is inversely proportional with eTh and these relations suggest that the radioelement distribution in these granites is at least in part governed by magmatic processes and that post magmatic uranium mobilization has occurred.

However, in the present work an attempt has been carried out to calculate the uranium migrated out or in the different lithologies utilizing the approach developed by the Chinese Bureau of Geology. Such an approach is based essentially on the fact that eU/eTh ratio is known for the same rock type or specific geologic unit in relatively closed environment. However, due to its high mobility uranium, under oxidizing condition, can be liberated and transported by oxidizing solution to reprecipitate, under favorable physico-chemical conditions, elsewhere. Thorium, on the other hand, being immobile, due to its stability under oxidizing condition, stay as it is in its original place and thus the U/Th ratio disturbed. This together with the very long half-life periods of U and Th lead to the assumption that the present thorium can be considered as original and that the uranium migrated, in or out the geologic unit can be calculated according to the following equations; $eU_m = eU_p - eU_o$; eU_m. ratio = $eU_m/eUp \times 100\%$; eU_o is the original or paleo uranium content and can be calculated as follow : eU_o =eTh content in specific rock type x the regional eU/eTh; According to these equations if; $eU_m > 0$ uranium is gained or migrated into the geologic unit; $eU_m < 0$ uranium is lost or migrated out from the geologic unit.

From above mentioned values (Table 3) we notice that the eU migrated out from G. Qash Amir (muscovite monzogranites), G. El Sella (two-mica monzogranites) and biotite tonalites, to the shear zone. The muscovite monzogranites lost about 20% of the present uranium, while the two-mica monzogranites lost about 180% and the biotite tonalites lost about 190% of their present uranium. In contrast, the shear zone acts as a good trap for the previous migrated uranium. Inside the shear zone itself, the jasper veins and argillic fine-grained granites gain uranium, whereas hematite fine-grained granites loss uranium.

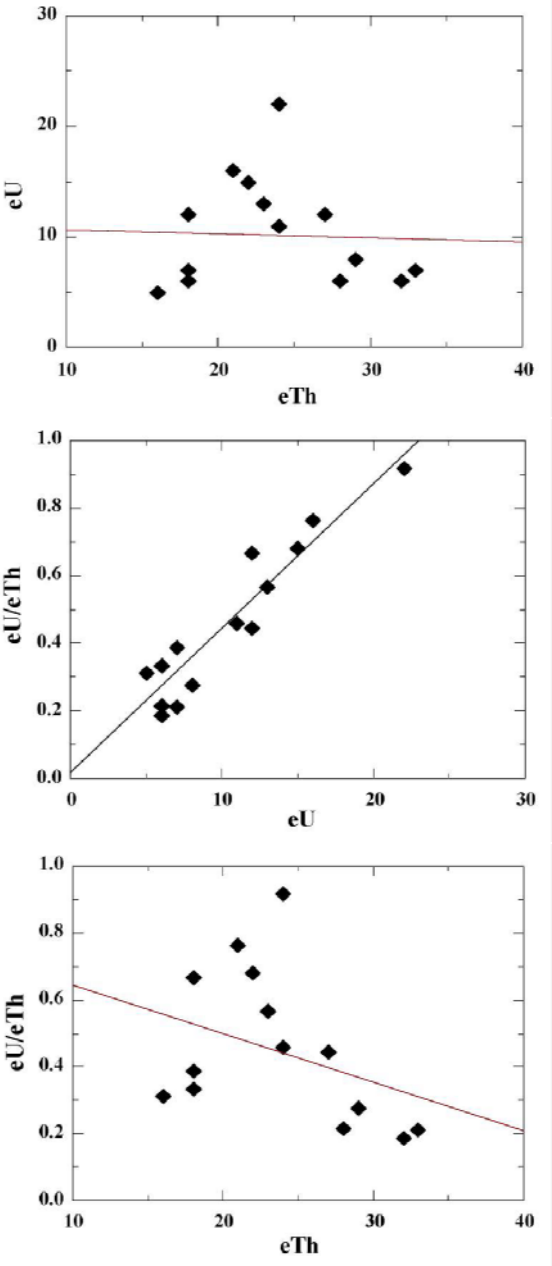

Fig. (4): The relation between eU-eTh, eU-eU/eTh and eTh-eU/eTh in two-mica monzogranites.

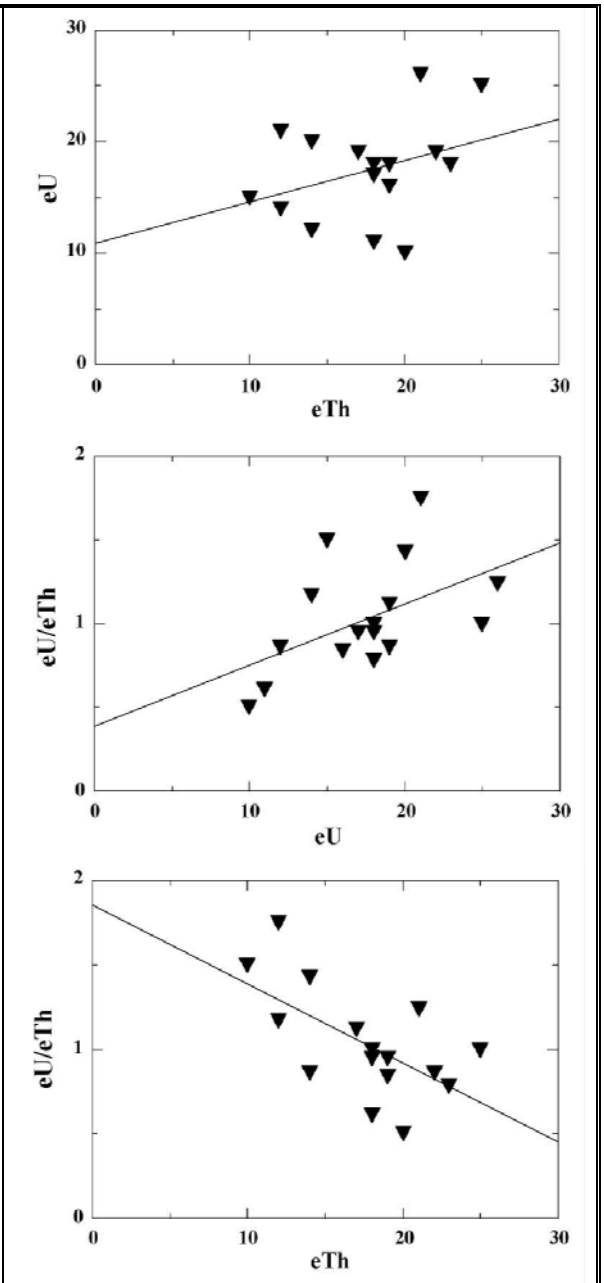

Fig. (5): The relation between eU-eTh, eU-eU/eTh and eTh-eU/eTh in muscovite monzogranites.

GEOCHEMISTRY

Chemical analysis were carried out for twenty five samples, collected from the study area, representing the older and the younger granitoid rocks. The analyzed samples include (five) samples from biotite tonalites and (six) samples from G. El Sella two-mica monzogranites, (twelve) samples from mineralized muscovite monzogranites of G. Qash Amir (two) samples from greisen and (two) samples from the shear zone. The results are given in Tables 4 and 5. The major oxides were analyzed by wet chemical techniques. The trace elements were determined by XRF techniques in Nuclear Materials Authority Lab.

A- Geochemistry of fresh granites

In comparison between G. Qash Amir (uraniferous muscovite monzogranite) and G. El Sella (fresh two-mica monzogranite), we found that, in case of major oxides, G. Qash Amir muscovite monzogranite showed high values of MgO, SiO_2, K_2O, CaO and Na_2O and depletion in Al_2O_3, TiO_2, P_2O_5 and total FeO_t in increasing order than G. El Sella two-mica monzogranites (Tables 4 and 5). In case of trace elements, G. Qash Amir displays high values of in Rb, Sc, Pb, Zn, Ga, Y and Nb while shows depletion in Ni, Cu, Co, Cr, V, Zr, Sr and Ba than G. El Sella in increasing order.

The biotite tonalite and two-mica monzogranite samples originated from metaluminous and peraluminous magma respectively (Fig. 6). The average chemical compositions of the investigated biotite tonalites and the two-mica monzogranitic samples are compared with different types of orogenic granitoids [11].

The biotite tonalite samples are orogenic and plot in the pre-plate collision (group 2) field [12]. The two-mica granite samples lie mostly in the syn-collision (group 6) regime (Fig. 7). The syn-collision group reflects the restricted range of "S-type" and anatectic granites [13]. suggested that the calc-alkaline granites are predominant in the syn-collisional related suites.

The Rb versus (Y+Nb) diagram [14] separated the four tectonic setting (Fig. 8). On this diagram the biotite tonalite samples fall in the VAG field, while the two-mica monzogranite samples lie in syn-col G field.

In the normative Qz-Ab-Or ternary diargam [15], the pressure isobars indicate formation under pressure varying between (1-5 kb) for the studied granitoid samples, while the temperature isotherms indicate temperature of crystallization between (670^o-800^o) for the two-mica monzogranites and $>840^o$ for the biotite tonalite (Fig. 9).

B- Geochemistry of altered granites

The uraniferous muscovite monzogranite and albitized monzogranite samples are plotted on the AKF ternary diagram (Fig. 10) [16] where A= K_2O, F = FeO^t+MnO+MgO and A = Al_2O_3-(Na_2O+K_2O). They show that, all uraniferous samples of G. Qash Amir muscovite monzogranite fall in sericite facies, while the two samples of the shear zone lie in argillic facies. Albitized granitic samples lie in K-silicate alteration facies, while the greisen samples lie in argillic facies.

According to the normative Qz-Ab-Or compositions, the altered granitic samples could be classified as sodic, potassic, silicic and greisen as shown in Fig. (11) [17]. Also the migration path of the minima of melts with increasing contents of fluorine in albitized granite than G. Qash Amir muscovite monzogranite samples, lie below the granitic eutectic temperature and exhibits a trend corresponding to crystallization in high P_{H2O} range (the range is from 0.5 to 3 k bar [18] and closely parallel to the trend A. The two shear zone samples plot parallel to silicic facies, whereas the greisen samples plot parallel to greisen trend.

Table (4): Major oxides (wt.%) and trace elements (ppm) of the biotite tonalites and two-mica monzogranites, El-Sella area.

Major Oxides	Biotite tonalites					Two-mica monzogranites					
	1R	**2R**	**3R**	**4R**	**5R**	**4**	**7**	**20**	**19**	**14**	**12**
SiO_2	70.73	69.70	70.02	68.90	70.12	70.13	72.75	70.88	71.78	72.35	72.77
TiO_2	0.24	0.26	0.28	0.21	0.24	0.21	0.11	0.11	0.11	0.10	0.13
Al_2O_3	12.52	11.80	12.20	12.86	11.90	14.54	13.35	14.64	14.43	13.91	13.84
Fe_2O_3	2.80	3.66	3.56	2.84	3.00	2.98	3.42	2.50	2.28	1.80	2.20
FeO	1.82	1.16	1.36	1.85	1.50	0.44	0.18	0.20	0.60	0.55	0.50
MgO	2.2	2.65	2.30	2.8	2.30	0.80	0.80	0.60	0.60	0.86	0.40
MnO	0.1	0.12	0.1	0.13	0.11	0.02	0.02	0.03	0.03	0.02	0.04
CaO	2.24	2.50	2.60	2.54	2.56	1.12	0.50	0.84	0.84	0.56	0.68
Na_2O	4.21	4.34	3.90	4.39	3.98	4.40	4.01	5.14	4.94	4.53	4.34
K_2O	1.30	1.31	1.42	1.6	1.62	3.53	3.19	3.25	3.55	3.26	3.31
P_2O_5	0.13	0.11	0.13	0.13	0.12	0.11	0.11	0.10	0.10	0.11	0.11
L.O.I.	0.96	0.98	0.86	0.98	0.78	1.28	0.30	0.37	0.34	0.93	0.91
Total	**99.23**	**98.55**	**99.01**	**99.50**	**99.95**	**99.54**	**98.72**	**98.63**	**99.57**	**98.96**	**99.19**
Trace elements											
Cr	15	15	22	18	16	70	86	92	124	81	95
Ni	2	2	4	4	2	5	9	8	11	9	9
Co	7	7	7	5	7	7	6	5	5	6	5
Sc	4	3	1	1	12	1	1	1	1	1	3
V	44	45	44	36	37	17	18	9	6	15	13
Cu	30	28	34	42	29	210	135	164	261	185	142
Pb	4	42	25	5	31	32	5	22	6	10	32
Zn	68	61	47	50	54	48	58	88	82	55	32
Rb	30	42	28	36	42	294	302	215	359	297	370
Ba	221	299	285	160	376	245	279	144	124	236	441
Sr	386	407	328	334	411	148	40	50	52	41	55
Ga	5	6	8	40	17	32	7	4	5	16	13
Nb	2	3	4	3	2	20	21	20	20	19	15
Zr	96	116	92	84	114	88	98	50	62	69	98
Y	11	13	5	12	14	12	8	13	14	10	19
Zr/Y	8.7	8.9	18.4	7.0	8.2	7.33	12.2	3.8	4.4	6.9	5.2
Zr/Sr	0.25	0.28	0.28	0.25	0.27	0.6	2.3	1	1.2	1.7	1.8
U	1.5	0.8	0.4	1.0	1.5	6	12	2	36	16	11
Th	2	2.5	3	3.5	2	28	27	14	32	21	24

Table (5): Major oxides (wt.%) and trace elements (ppm) of the mineralized and altered rocks.

Major	Muscovite monzogranite						Albititic granite				Argilic		Greisen	
Oxides	37	34	38	39	35	28	33	61	58	59	16	17	48	49
SiO_2	71.43	70.85	71.94	73.15	73.49	74.10	71.75	75.01	71.88	72.91	69.41	71.50	78.24	79.98
TiO_2	0.11	0.11	0.11	0.10	0.17	0.10	0.11	0.17	0.13	0.11	0.24	0.22	0.08	0.02
Al_2O_3	14.78	14.94	14.78	13.59	13.61	13.52	13.91	11.11	13.41	11.91	14.95	13.22	12.69	11.98
Fe_2O_3	1.9	2.8	1.87	0.10	2.14	1.20	2.32	2.43	1.26	2.80	5.08	4.42	0.63	0.82
FeO	0.28	0.36	0.12	0.76	0.24	0.36	0.44	0.52	0.32	0.36	012	0.24	0.3	0.28
MgO	0.80	0.80	0.80	0.80	0.60	0.60	0.80	0.60	1.00	0.40	0.8	0.60	0.21	0.25
MnO	0.13	0.16	0.1	0.12	0.13	0.2	0.21	0.12	0.1	0.1	0.12	0.13	0.06	0.05
CaO	0.84	1.12	0.84	0.56	0.84	0.84	0.84	0.84	0.84	1.12	1.68	1.12	0.58	0.63
Na_2O	4.06	4.61	5.27	4.33	4.25	4.71	5.14	5.94	6.27	6.27	0.68	0.67	0.83	1.3
K_2O	3.89	3.80	3.44	3.31	3.49	3.37	3.39	3.26	3.96	3.49	2.56	2.59	2.98	2.5
P_2O_5	0.10	0.10	0.10	0.10	0.10	0.10	0.10	0.10	0.10	0.10	0.10	0.11	0.06	0.06
L.O.I.	0.49	0.53	0.48	0.46	0.37	0.44	0.80	0.11	0.19	0.28	03.49	3.45	2..3	2.2
Total	98.84	99.74	99.81	98.15	99.09	99.22	99.37	100.2	100.1	99.47	99.04	99.85	99.55	100.1
Cr	35	69	84	77	29	76	31	143	91	93	137	16	19	20
Ni	10	9	11	7	7	7	8	10	11	7	11	6	3	3
Co	5	7	6	5	5	5	5	5	5	5	5	3	3	3
Sc	1	2	3	1	1	1	1	1	1	2	1	1	-	--
V	7	13	8	8	8	32	7	7	6	5	7	9	5	5
Cu	190	123	331	234	177	181	186	77	141	136	77	33	22	20
Pb	44	14	5	10	35	4	50	20	23	18	32	52	29	28
Zn	163	77	110	93	103	119	166	99	51	55	93	12	218	203
Rb	386	460	430	331	335	477	410	472	406	388	375	410	760	616
Ba	37	119	102	89	70	14	20	16	39	37	15	108	296	288
Sr	36	89	41	42	48	35	37	28	30	26	25	50	52	45
Ga	24	17	32	20	19	29	21	23	29	20	16	14	57	49
Nb	81	61	97	102	124	414	101	54	62	55	66	87	27	29
Zr	31	51	39	49	49	115	36	81	67	65	57	39	65	49
Y	46	56	50	40	49	91	46	49	42	41	38	50	21	17
Th	28	22	12	14	19	35	17	10	12	15	377	126	14	13
U	48	35	21	20	41	125	19	15	14	30	80	11	20	15

DISCUSSION AND CONCLUSIONS

Among the different rock units in the G. El Sella area, the two-mica monzogranite and muscovite monzogranite are the most favourable host rocks for uranium and thorium mineralization. The muscovite monzogranites (G. Qash Amir) are affected by deutric alteration and characterized by gradational contact with two-mica monzogranite (G. El Sella), peraluminous in nature with visible primary and secondary uranium minerals + beryl + columbite and without shearing or channel ways for mobilization of uranium. The peraluminuos two-mica monzogranites are emplaced during syn-collision regime, and without visible uranium minerals but dissected by major shear zone (ENE-WSW) which considered as a good trap for uranium.

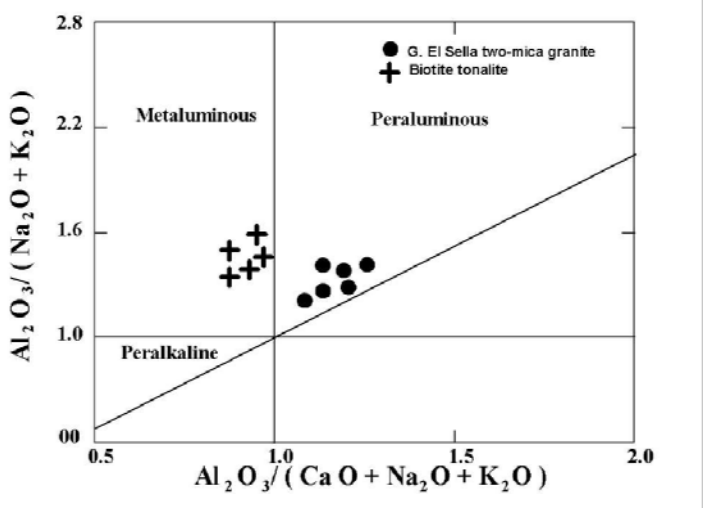

Fig. (6): Al_2O_3 / (Na_2O + K_2O) - Al_2O_3 / (Ca + Na_2O + K_2O) binary diagram [11].

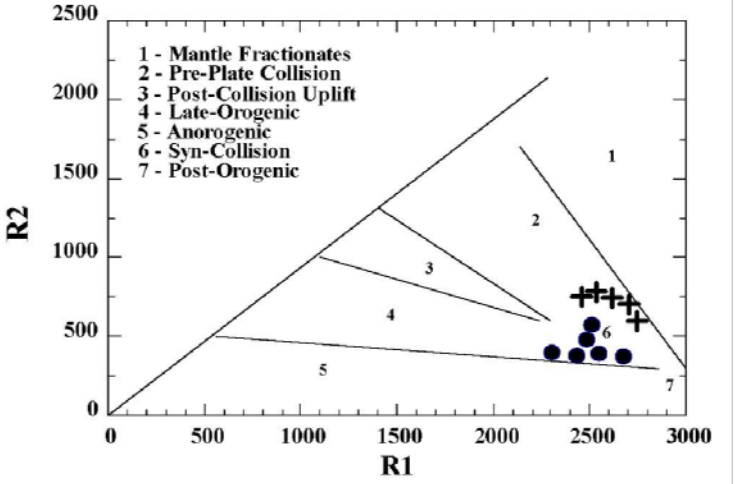

Fig. (7): R1-R2 diagram [12].

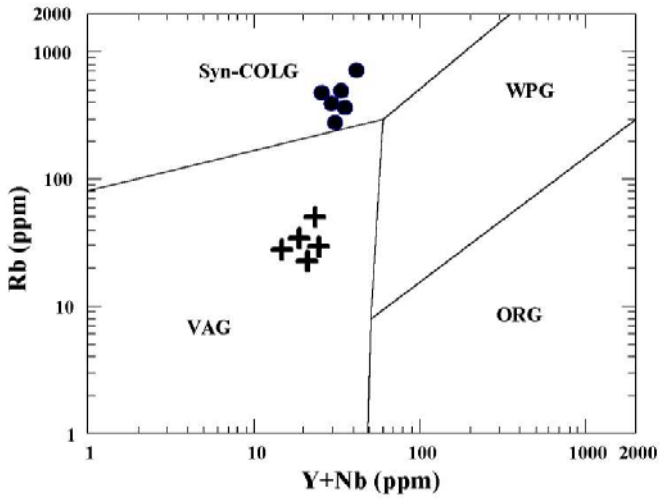

Fig. (8): Rb-(Y+Nb) diagram [14].

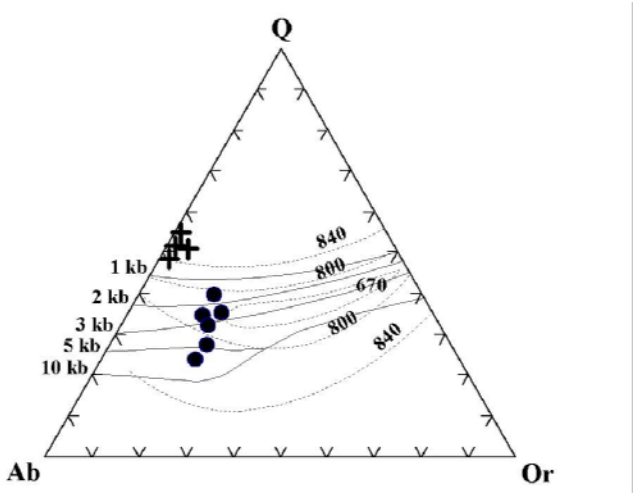

Fig. (9): Normative Q-Ab-Or ternary diagram for temperature and pressure [15].

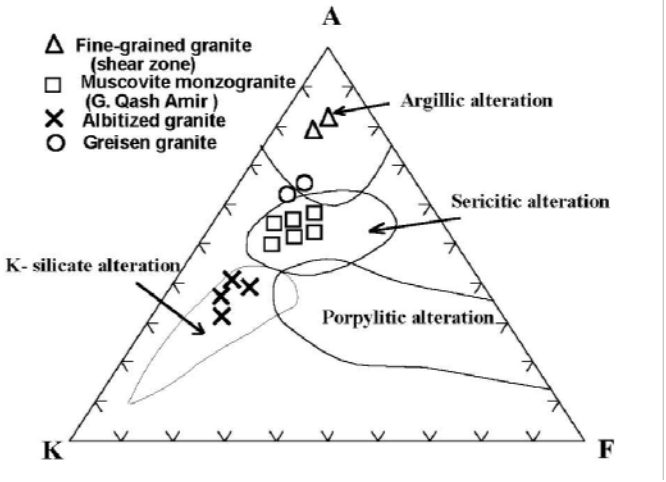

Fig. (10): AFK diagram [16].

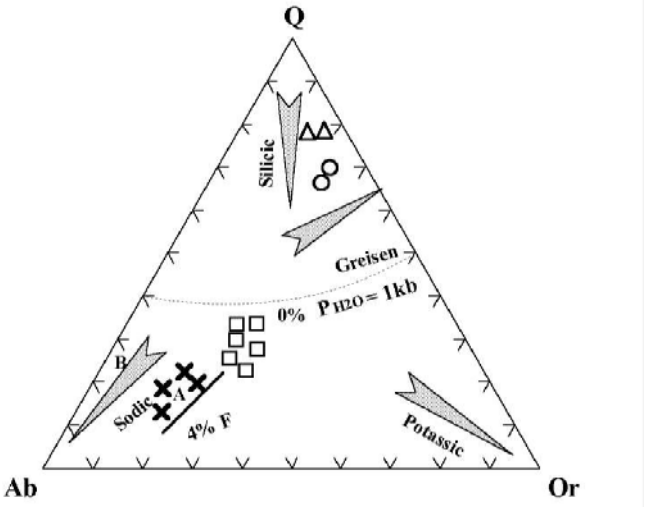

Fig. (11): Normative Qz-Ab-Or ternary diagram of the altered granites.

El Sella shear zone is subdivided by two wrench faults (N15^{o}W – S15^{o}E) into three separated parts. The relief decreases from the third part to the first part of the shear zone. So, the original uranium was migrated from the high relief and leached by circulated meteoric water through the ENE-WSW channelways and concentrated in the lower shear zone parts (second and first parts). This could be illustrating the lower eU- and higher eTh-contents in the hematitized third part. The eU/eTh ratio ranges from 7 – 55 in the first part, through 5.5 – 38 in the second part to 4 – 36.6 in the third shear zone part with average (hematitization part is excluding) equal to 13.3, post magmatic redistribution of U is suggested and this could be a favorable economic criteria because U concentrated into a deposit within the shear zone.

The vein type (G. El Sella shear zone) is considered as a good trap for uranium mineralization for the following factors:

1-The high eU contents of both the fertile two-mica monzogranites and the muscovite monzogranites (G. El-Sella and G. Qash Amir respectively).

2- The high average of eU/eTh ratio in El Sella shear zone (13.3)

3- A wide barrier of silica vein (2-10m) in El Sella shear zone.

4- The post-magmatic activities are represented by microgranite, dolerite and latite dykes.

5- The chemical trap in El Sella shear zone is represented by basic dykes and tertiary olivine basalt, as well as mafic–ultramafic blocks are in close contact with the shear zone.

6- Tectonically, the fault trends NW-SE and NNW-SSE played at least a role in the remobilization of uranium along the shear zone.

7- The reducing environment is represented by sulphide minerals and carbonate (calcite pockets).

8- Argillization, hematization, fluoritization, sulphidization and silicification are the main alterations variety containing visible U-minerals.

REFERENCES

[1] International Atomic Energy Agnecy, 1999, Gamma-ray surveys in uranium exploration. Technical report series 186 Vienna, 89 p.

[2] Cuney, M., 1987, Metallogenesis of uranium deposits. IAEA, Vienna.

[3] Streckeisen, A., 1976, To each plutonic rock its proper name. Earth Science Reviews, Vol. 12, 1-33 p.

[4] El Agami, N. L., Abu Baker, M. A., Ibrahim, M. E. and Rashed, M. A., 1999, Mineralogical and geochemical studies for the mineralization of Halaib area, South Eastern Desert, Egypt. J. Geol. Sc., 43/1, p. 27-38.

[5] Assaf, H. S., Ibrahim, M. E., Amar, S. E., Shalaby, M. and Rashed, M. A., 1999, Geological and mineralogical studies on the radioactive mineral occurrence at Qash Amir area, Southeastern Desert, Egypt. Egypt. Min, 11, p. 135-156.

[6] Adams, J. A. S., Osmond, Y. K., and Rogers, J. J. W., 1959, The geochemistry of thorium and uranium, physics and chemistry of the Earth, 3, Pergamon Press, London.

[7] Turkian, K. K., and Wedepohl, K. H., 1961, Distribution of the elements in some major units of the earth's crust. Geol. Soc. Am. Bull., 72, 175-192 p.

[8] Clarke, S. P., Peterman, Z. E. and Heier, K. S., 1966, Abundance of uranium, thorium and potassium, In: S. P. Clarke 4, J (Editor), Handbook of physical contants, Geol. Soc. Am. Mem.97, section 24,521-541 p.
[9] Rogers, J. J. W., and Adams, J. A. S., 1969, Uranium and thorium, In : Handbook of Geochemistry, Vol. II-3, 92-B-1 to 92-0-5 and 90-B-1 to 90-0-5 (ed. K. H. Wedepohl), Springer Verlag, Berlin.
[10] Boyle, R. W., 1982, Geochemical prospecting for thorium and uranium deposits. Develop. Economic, Geol., Vol. 16, El Sevier, Amsterdam, 489 p.
[11] Maniar, P. D., and Piccoli, P.M., 1989, Tectonic discimination of granitoids. Geol. Soc. Am. Bull., 101, p. 635-643.
[12] Batchelor, R. A. and Bowden, P., 1985, Petrogenetic interpretation of granitoid rock series using multicationic parameters. Chemical Geology, 48, p. 43–55.
[13] Stoeser, D. B. and Elliott, S. E., 1980, Post-orogenic peralkaline and calc-alkaline granites and associated mineralization of the Arabian Shield, Kingdom of Saudi Arabia, In: Al-Shanti, A. M, Ed., Evolution and mineralization of the Arabian-Nubian Shield: Inst. Appl. Geol. King Abdel Aziz Univ., Jeddah, Bull. 2, 1-23 p.
[14] Pearce, J. A., Harris, N. B. W., and Tindle, A. G., 1984, Trace element discrimination diagrams for the tectonic interpretation of granitic rocks. J. Petrol., V. 25, 956-983p.
[15] Tuttle, O. F., and Bowen, N. L., 1958, Origin of granite in the light of experimental studies in the system $NaAlSi_3O_8$-$KalSi_3O_8$-SiO_2-H_2O. Geol. Soc. Am. Em., 74, 153p.
[16] Meyer, C., and Hemley, J. J., 1967, Wall rock alterations, 166-235. In : Geochemistry of hydrothermal ore deposits (H.G. Barnes, ed.), Winston Inc. New York, 670 p.
[17] Stemprok, M., 1979, Mineralization granites and their origin. Episodes, 3, p. 20-24.
[18] Winkler, H. G. F., Boese, M., and Marcoponlos, T., 1975, Low temperature granitic melts. Neues Jahrbuch fur Minerologie Montatshefte, 6, p. 245-268.